2020 8th IEEE International Conference on Biomedical
Robotics and Biomechatronics (BioRob)
New York, USA. Nov 29 - Dec 1, 2020

A Soft Inflatable Wearable Robot for Hip Abductor Assistance: Design and Preliminary Assessment

Hee Doo Yang, Myles Cooper, Tunc Akbas, Lexine Schumm, Dorothy Orzel, and Conor J. Walsh

***Abstract*— In this paper, we present the design, characterization and preliminary testing of a soft inflatable wearable device that can apply assistance in parallel with a wearer's abductor muscles. The device is composed of a three-piece textile suit with and integrated textile-based inflatable hip abduction actuator (HAA) that can produce an assistive torque about the hip in the frontal plane when pressurized. We characterize the torque output of the device at multiple hip obliquity angles and pressures using an instrumented mannequin, and show that the device achieves a maximum torque of ∼14 Nm at 345 kPa. A proof of concept, single subject test was performed to evaluate the ability of the wearable device to assist hip abduction during single leg stance by monitoring abductor muscle activity. At the high assistance (≈14% of biological hip moment), the device reduced the measured muscle activity in gluteus medius (30%), gluteus maximus (43%) and tensor fasciae latae (37%) compared to a condition without assistance during single leg stance. These results demonstrate potential for the soft inflatable wearable device to provide assistive hip abduction torque during walking in order to improve reduced lateral stability caused by muscle weakness.**

I. INTRODUCTION

The age of the American population is rising; the number of people aged 65 and over was 50.9 million in 2017 and the number is expected to reach 94.7 million in 2060 [1]. As people age, most older people face difficulties with mobility [2]. This in turn limits engagement in both physical and community activities amongst the elderly [3], which leads to a lower quality of life [4], [5]. Mobility loss may also increase the chance of falling [6], which can lead to injury and reduce life expectancy [7], [8]. One of the major contributors of reduced mobility is the loss of muscle mass over time (1-2% per year over the age of 60) that occurs with aging [9]. One possible way to provide assistance to weakening muscles is through robotic exoskeletons, which have been shown to improve mobility-related tasks like walking [10].

Over the past decades, various wearable robotic devices have been developed to assist the lower extremities. Advances in actuator performance and control systems have enabled many tasks requiring full leg assistance including lifting heavy loads [11], [12], assisting wearers to walk [13], and rehabilitation to regain mobility [14], [15]. More recently, wearable robots that assist a single joint (e.g. hip, knee or ankle) have been developed to understand their individual contributions to walking [10], [16], [17], [18], [19], [20]. Among the variety of exoskeletons in development, soft robotic wearable systems combine robotic systems with soft materials to apply forces to the body that assist muscles. These soft exoskeletons usually come to deliver less assistance compared to traditional exoskeletons due to the lack of rigid components, but they tend to be lighter weight and more compliant [10], [19], [20]. By using actuation methods such as pneumatics or cable-drive systems rather than linkages and motors, they are also less reliant on alignment with joints of the body, making them potentially safer and more comfortable. Soft wearable devices developed to date have been able to augment the work of natural muscle to reduce metabolic cost [19], [21] or assist with walking after stroke [10].

Despite recent advancements, existing soft robotic systems for the lower extremities do not address hip abduction, which is crucial to maintain lateral stability during walking [22], [23]. The hip abductors generate contralateral torque against the body's center of mass (COM) and stabilize pelvic angle during the single stance phase of walking. As people age, due to muscle loss, the amount of torque produced by the hip

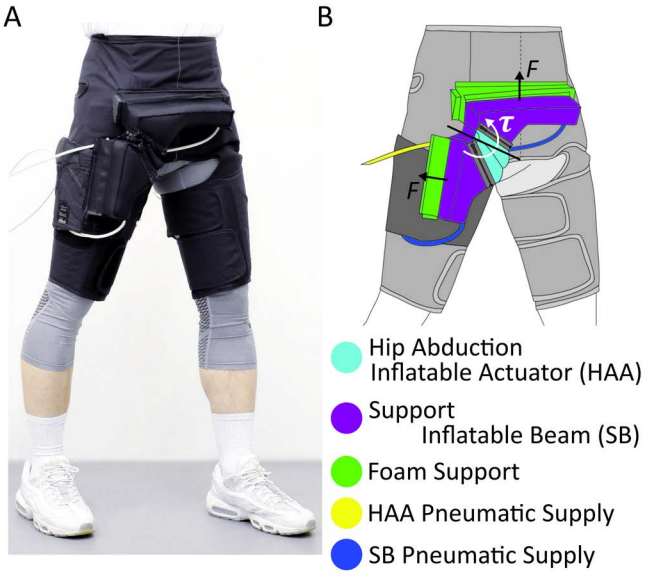

Fig. 1. Design Overview; A) picture of the wearable robot on person; B) schematic figure of the wearable robot with detailed components: a hip abduction inflatable actuator (HAA), a support inflatable beam (SB), a foam support, and pneumatic supplies for HAA and SB.

This study is based upon work supported by the Office of Naval Research (ONR) award number N00014-17-1-2121, the Wyss Institute for Biologically Inspired Engineering and the John A. Paulson School of Engineering and Applied Sciences at Harvard University.

H. Yang (e-mail: hdyang@seas.harvard.edu), and C. Walsh (e-mail: walsh@seas.harvard.edu) are with the John A. Paulson School of Engineering and Applied Sciences and the Wyss Institute for Biologically Inspired Engineering, Harvard University, Cambridge, MA 02138 USA

abductors is reduced by 20-40% [24]. This limits the ability to properly perform hip abduction to stabilize the pelvis, which results in lateral instability and can lead to potential issues such as Trendelenburg gait [25]. Weakness of the hip abductors also increases gait variability including step time and step width, which was correlated with risk of falls [26], [27].

Some rigid exoskeletons have been studied to assist the hip abductors for lateral stability. These exoskeletons provide additional torque to the hip joint in the frontal plane, which shifts the center of mass (COM) to maintain balance during walking [28], [29]. Soft robotics offers a possible way to give assistance with low weight and low impedance to natural movement. In order to achieve hip abductor assistance in the frontal plane, a device should meet the following requirements: soft and lightweight for low restriction of mobility, and sufficient torque to reduce muscle activity.

We propose a soft inflatable robot to assist the hip abductor muscles by applying a torque to the hip joint that complements the hip abductors' natural function. The device has lightweight textile suit components and a low air volume design. In this paper, we introduce the design of the wearable device in detail in Section II. In Section III, we describe device characterization using the hip mannequin. Finally, In Section IV, we present our preliminary testing on a single healthy subject and analyze EMG reduction to quantify the impact of the device on hip abductor muscle activity.

II. A Soft Inflatable Wearable Robot for Hip Abductor Assistance

The aim of this paper is to understand the impact of the proposed device on hip abductor muscle activity. The long-term goal of this research is to create a soft wearable robotic device to apply assistance to support the hip abductor muscles during walking. However, in a system used for walking, the rate at which torque is applied to the body and the timing of assistance need to be tightly controlled. To avoid this additional complexity, our initial prototype is intended to apply an abduction torque assistance while a subject is standing on one leg, without considering actuator dynamics and controls.

A. Design considerations

Design requirements are considered based on the walking condition. To understand what percentage of normal biological torque to apply with the device, we can look to a recent simulation study that shows hip abduction assistance while walking with a heavy load may result in high metabolic cost reductions (12.9%) with relatively lower assistive power (0.42 $\pm$ 0.11W/kg) [30]. Additionally, for ankle assistive devices that have shown promising EMG or metabolic reductions, assistance levels have ranged from 10-30% of biological joint torque [31]. Considering the relative assistance efficiency of the hip abduction compared to ankle plantarflexion, we set the desired assistance goal to be at least 10% of natural biological joint torque. Given the reported measurements of hip abduction of $\sim$1 Nm/kg during normal walking [32], we set a design requirement for the device of 0.1 Nm/kg. Thus, assuming weight of a subject of 86 kg, this relates to a torque requirement of 8.6 Nm.

To assist with hip abduction without restricting the user from walking, an additional requirement for the device was to allow a range of motion of at least 5 degrees of hip abduction and 5 degrees of hip adduction ($\pm$ 5° in the frontal plane), and at least 30 degrees of hip flexion and 10 degrees of hip extension ($+30°/-10°$ in the sagittal plane) [33]. Another goal was to minimize the volume of air necessary to inflate an actuator. Doing so would lessen the delay between commanded pressure and torque generation, resulting in a faster response time and possibly providing a future path to creating portable systems.

B. Design overview

The device design is shown in Fig. 1A. To provide assistive torque, a hip abduction actuator (HAA) is inflated, generating a torque that is transmitted through two support beams which were sewn into a custom textile suit which then exerts force on the femur and pelvis as shown in Fig. 1B. The HAA and support beams are inflatable structures that are airtight and hold pressure at 413 kPa. To withstand high pressure, the HAA and the support beams were made of inextensible fabric (Weathermax, USA), which is a high-stiffness woven

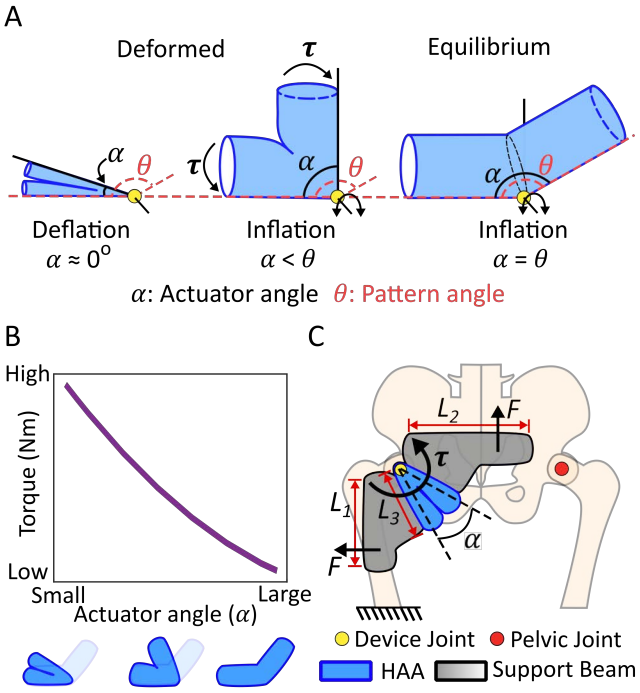

Fig. 2. Actuation principles; A) a schematic figure of the hip abduction actuator (HAA). The angle (α) is the current actuator angle (deformed), and the angle (θ) is the pattern angle as the maximum unfolding angle (equilibrium). The actuator is folded when deflation ($\alpha \approx 0$), and then the actuator exerts torque while attempting to inflate to the pattern angle due to force equilibrium when inflation; B) a theoretical torque profile related to the different actuator angle (α); C) a simplified diagram of the HAA, the support beams, and the pelvis system. The support beams react against the femur (fixed) to provide torque from the HAA to the pelvis.

textile, with an internal TPU bladder (#HM65-PA, Perfectex LLC.) to provide air impermeability.

To transfer assistive torque provided by the HAA to the wearer, one support beam is sewn on top of an actuating sleeve, and another support beam is sewn on top of a thigh wrap in Fig. 3C. The intent of the support beams is to have them inflated initially (to 103 kPa) when the device is intended to assist user (e.g. during locomotion) and held at that pressure. These features assist in transferring torque provided by the HAA to the user. Additionally, the HAA is attached with support beams through zippers to enable them to be being easily replaceable. The HAA's pressure can be modulated to control the level of assistance applied to the wearer. A simplified schematic is shown to describe the HAA's actuation principle in Fig. 2A and how forces from the HAA with compressed air transfer to the wearer in Fig. 2C.

C. Actuation principles

The actuation mechanism of the HAA, shown in Fig. 2A and 2B, is the same as that of other buckling cylindrical actuators described previously [34]. This type of actuator consists of two intersecting cylindrical surfaces that are sewn at some pattern angle (θ) that defines the angle between those cylinders when the actuator is fully inflated. The HAA is folded to an actuator angle ($\alpha \approx 0$) when it is deflated, and rotates about a fixed axis when the HAA is pressurized. As the HAA inflates, the HAA exerts torque until the actuator angle reaches the pattern angle ($\alpha = \theta$) to re-establish equilibrium. As the actuator angle (α) increases, the actuator produces lower torques at a given pressure as described in Fig. 2B.

This operating principle of the HAA can be used to help understand the function of the wearable device as shown in Fig. 2C. We model the femur and pelvis as independent rigid bodies which are linked by a revolute joint in the frontal plane. We treat the femur as our fixed reference frame and think of torque produced by the HAA as being applied to the pelvis: the HAA generates torque according to its current actuator angle (α), and the torque is transferred through the support beams and suit to the pelvis in Fig. 2C.

D. Design principles

1) Secure attachment on the body: In order to assist the hip abductor muscles, the torque generated by the HAA acts on the femur and pelvis. To achieve this, (i) the device secures each end of the actuator to the thigh and waist, respectively. (ii) We also wanted to align the center of rotation of the HAA with the center of rotation of the hip joint from the frontal view to transmit torque efficiently. In order to address anchoring and alignment separately, we made the suit in three pieces (Fig. 3A and 3C): an anchoring sleeve, an actuating sleeve, and a thigh wrap. The anchoring sleeve provides a tight fit of the suit on the body. The actuating sleeve and the thigh wrap can be easily connected to the anchoring sleeve and adjusted such that the HAA rotates concentric with the hip joint in the frontal plane.

To anchor the device to the hip, we designed the anchoring sleeve with two parts: a pelvic part and a femoral part as shown in Fig. 3C. First, the anchoring sleeve is tightly fastened around the hip to increase friction between the two to transmit the force from the HAA to the pelvis. However, the waist increases in diameter in the downward

Fig. 3. Design principles; A) a picture of the device with three different components: an anchoring sleeve, an actuating sleeve, and a thigh wrap; B) a schematic figure describing a role of the wedge-shaped foam piece to prevent from outward expansion; C) detailed three components: first, the anchoring sleeve (blue) is tightened around the hip, and then the actuating sleeve (yellow) and the thigh wrap (red) anchor to the anchoring sleeve via hoop and loop fasteners; D) the actuator angle (α) requirement at neutral angle of 0°. The support beam is attached on the femur. The support beam moves with the same angle in the frontal plane as hip ab/adduction angle. The minimum actuator angle relates to the maximum adduction angle.

direction on the body, making it ill-suited to react against an upward force. The thigh, however, gets larger in diameter as it progresses upward from the knee, making it better for resisting upward force, so we added a thigh part to the anchoring sleeve to provide more resistance against the upward force of the actuator.

Next, in order to efficiently use the torque from the HAA to assist hip abduction, we wanted to ensure that the center of rotation of the actuator was roughly coaxial with the center of rotation of the pelvic joint when viewed from the frontal plane. To do this, we attached the actuating sleeve to the anchoring sleeve via hook-and-loop fastener so that it can be positioned anywhere on the pelvis relative to the anchoring sleeve and could be fit to multiple hip geometries. The thigh wrap is installed to the femoral part of the anchoring sleeve to achieve the same level of adjustability.

2) Maximize torque generation of the HAA: As seen in Fig. 2C, the torque generated by the HAA increases as the actuator angle (α) decreases. To take advantage of this, our design goal was to keep the actuator angle (α) at a minimum throughout its range of motion. This minimum is bounded, however, by the average 30° range of motion of the hip in adduction, as described in Fig. 3D (right) [35]. To avoid flattening the HAA completely (α = 0), the HAA was mounted such that, at the frontal plane neutral angle, the angle (α) of the actuator is greater than 30°. We chose to set the actuator angle (α) of 40° at the neutral angle to account for the thickness of the actuator as shown in Fig. 3D (center) and designed the support beams to match the requirement.

Additionally, to prevent inefficient torque transmission, the device had to be geometrically constrained to avoid buckling of the HAA upon inflation. When viewed from the sagittal plane, the support beams can be seen to be attached only to the sleeves on the side proximal to the body, as shown in Fig. 3B (left). To maximize abduction torque transmitted to body, we added wedge-shaped foam pieces pictured in Fig. 3B (right) to bias the uninflated orientation of the actuator to be rotated inward as viewed from the sagittal plane. This pre-rotation of the HAA in the sagittal plane corrects for the natural expansion of the actuator such that it is in a more aligned to the frontal plane when inflated.

III. Actuator Characterization

A test rig was constructed to perform an experiment to understand how much torque the hip wearable device could apply to the pelvic joint. We investigated the relationship between the internal pressure difference of the HAA and the torque output.

A testing mannequin, pictured in Fig. 4A, was created that contains two revolute joints between plastic waist and plastic thigh components. The size of the thigh and waist pieces were made to match measurements of a lab member for an initial wearable prototype was developed. The test mannequin includes two load cells (Futex LTH-300) to measure the static force output of the mannequin in the frontal and sagittal planes. The angles of the joints are manually set about each axis with a pair of lead screws. The range of motion was constrained between -10 and 10 degrees in the frontal plane to cover beyond the normal range of motion of the hip in the frontal plane. To more easily analyze how the device assists the hip abductors, the angle in the sagittal plane was kept at 0°, and frontal plane torque was measured. An offboard pneumatic system was used to control air pressure during testing. The system contains an electronic regulator (ITV1051-21N2BS4, SMC, Japan), a pressure sensor (100PGAA5, Honeywell, USA), DAQs (NI6733 NI6259, National Instruments, USA), and xPC Target (Mathworks, USA). The system was operated

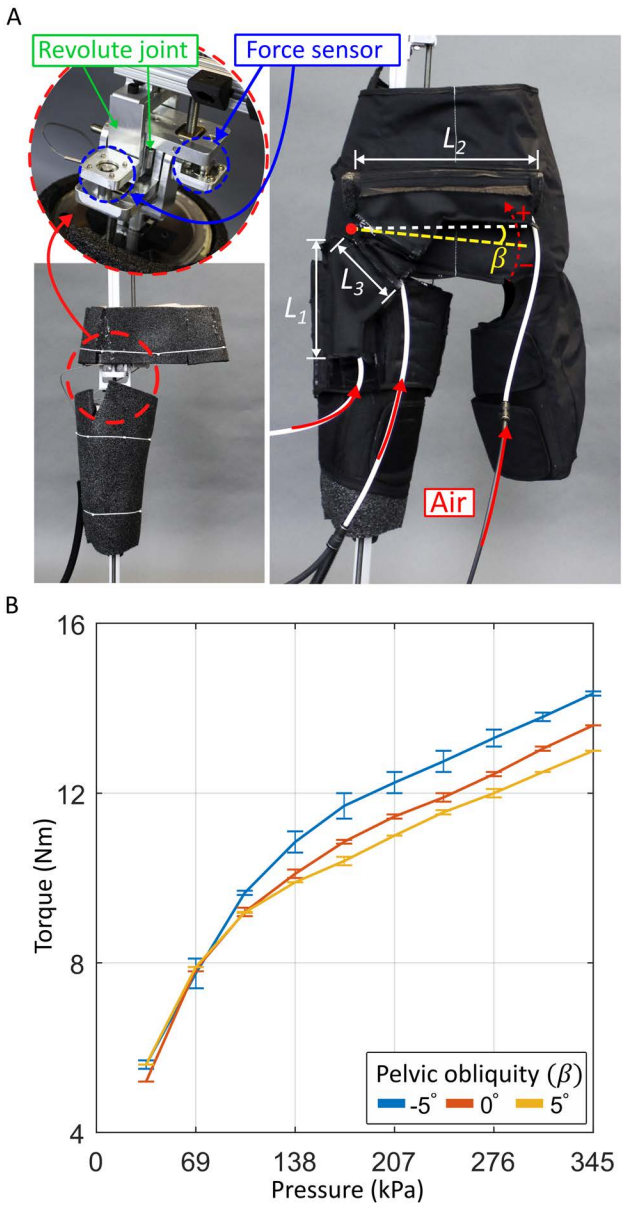

Fig. 4. Results from experiments showing how the torque output, the angle range of the pelvic and the pressure difference are related; A) Hip device test mannequin: It contains two revolute joints to mimic normal hip range of motion and two force sensors to measure forces produced by the hip abduction actuator (HAA); B) The relationship between the pressure difference and the torque output (Mean ± SD) with different pelvic obliquity (β=-5, 0, 5 degrees). The test was conducted for each condition twice.

using Simulink (Mathworks, USA), recording analog signals at 500Hz.

The HAA was made with diameter of 5 cm and L_3 = 8 cm in Fig. 4A. Additionally, the support beam was fabricated with L_1 = 16 cm and L_2 = 25 cm. To test the device, it was first installed on testing mannequin at a hip angle of 0° and the support beams were inflated to 103 kPa (15 PSI). Then, the HAA was inflated to 34.5 kPa (5 PSI), held at pressure for five (5) seconds, and deflated back to 0 kPa. This was repeated at up to a pressure of 345 kPa (50 PSI) in increments of 34.5 kPa (5 PSI). For each pressure, the average torque output during the last two and a half (2.5) seconds of held pressure was plotted in Fig. 4B. This test was conducted with three different angles of pelvic obliquity (frontal plane rotation of pelvis) (β: -5, 0, and 5) were measured, which represent the average hip range of motion during walking. The test was run twice at each angle β. According to Fig. 4B, the device generates 13-14 Nm of torque at 345 kPa, which is 14-16% of natural hip abductor torque (1 Nm/kg) based on a subject weight of 86 kg. In order to provide the goal of 10% of biological torque (8.6 Nm), the device needed between 69 kPa and 103 kPa. The deviations in torque measured at $\beta = -5°$ may have been caused by the suit shifting slightly on the mannequin during testing.

IV. Human subject experiment

A. Experimental protocol

A single subject study was performed on a healthy individual to evaluate the capability of the device to provide lateral support by reducing muscle effort from the hip abductors. Peak force generation of the hip abductor muscles is observed during early and mid-stance phases of walking to provide mediolateral stability [30]. To resemble this phase, sagittal plane motion was eliminated, and frontal plane motion was separated into dynamic and static parts. The static part (relating to the mid-stance phase) was simulated by standing on one foot (single support). The dynamic part (relating to the early single support phase) was simulated by transitioning from double support to single support. For each activity, three conditions were implemented: unpowered (HAA unpressurized), low assist (HAA pressurized to 138 kPa, ≈11.5% of biological joint torque), and high assist (HAA pressurized to 276 kPa, ≈14% of biological joint torque). The pressurisation was triggered manually by researchers. For all conditions the support beams were inflated a constant pressure of 103 kPa. Each activity started in a double leg stance posture with the right foot located higher than the left foot (≈5 cm) and the subject was asked to move to a single leg stance by lifting the left foot to match the height of the right foot. For the steady activity, the HAA was pressurized five seconds after transitioning from double leg stance to single leg stance and the evaluation of the steady state started five seconds after HAA was inflated. Data were collected for five seconds (standing trial, Fig. 5A). For the dynamic activity, the HAA was pressurized during the transition from double leg stance to single leg after toe-off and data were collected for one and a half seconds (dynamic trial, Fig. 5B). Data for the unpowered condition were collected at the same time interval matching the standing and dynamic trials. Each condition was evaluated two times within each trial. During each trial, the participant was allowed to lightly touch an instrumented handrail to avoid additional postural sway by lack of somatosensory information [36]. All study procedures were approved by the Harvard Medical School Institutional Review Board.

B. Data collection and processing

The surface electromyography (sEMG) sensors (Delsys, Natick, MA, USA) were placed on the gluteus medius (GMed), gluteus maximus (GMax), tensor fasciae latae (TFL) and erector spinae (ES) of the weighted limb. The selected gluteal muscles and TFL were selected to assess the support of the device on hip abductors, whereas the ES was selected to evaluate the probable postural adjustments on the lumbar spine. The vertical toe displacement on the unweighted limb and pelvic obliquity were recorded with an optical motion capture system (Qualisys, Gothenburg, Sweden) using reflective markers placed on anatomical bony landmarks on foot and pelvis segments. Possible additional postural adjustments of the participant in the frontal plane were assessed by measuring peak toe height (the vertical toe marker displacement) and maximum increase in pelvic obliquity for the standing and dynamic trials for each condition, as shown in Table I. The contact forces of the finger touch were collected with an instrumented handrail (Bertec, Columbus, OH, USA) to verify the handrail was not used as a body weight support during any activities. EMG and force signals were recorded at 2kHz and the motion capture data was recorded at 120Hz. During post-processing, the raw EMG signals were filtered with a fourth-order band- pass Butterworth filter with cutoff frequencies of 20–400 Hz in order to remove electrical noise and biological artifacts, recti-

TABLE I

Handrail forces and kinematic measures (MEAN ± SD), for two sessions during each condition in standing and dynamic trials

Activity	Condition	$F_{handrail}$ (N)	Max. Pelvic Obliquity (deg)	Peak toe height (cm)
Standing trial	Unpowered	9.12 ± 0.86	1.21 ± 0.11	6.74 ± 0.03
	Low assist	8.94 ± 0.08	1.95 ± 0.10	6.49 ± 0.14
	High assist	9.76 ± 1.42	0.95 ± 0.31	6.52 ± 0.15
Dynamic trial	Unpowered	6.62 ± 5.68	2.67 ± 1.20	4.01 ± 0.29
	Low assist	6.28 ± 0.91	2.54 ± 0.15	3.92 ± 1.20
	High assist	5.58 ± 1.64	3.50 ± 0.70	3.46 ± 0.76

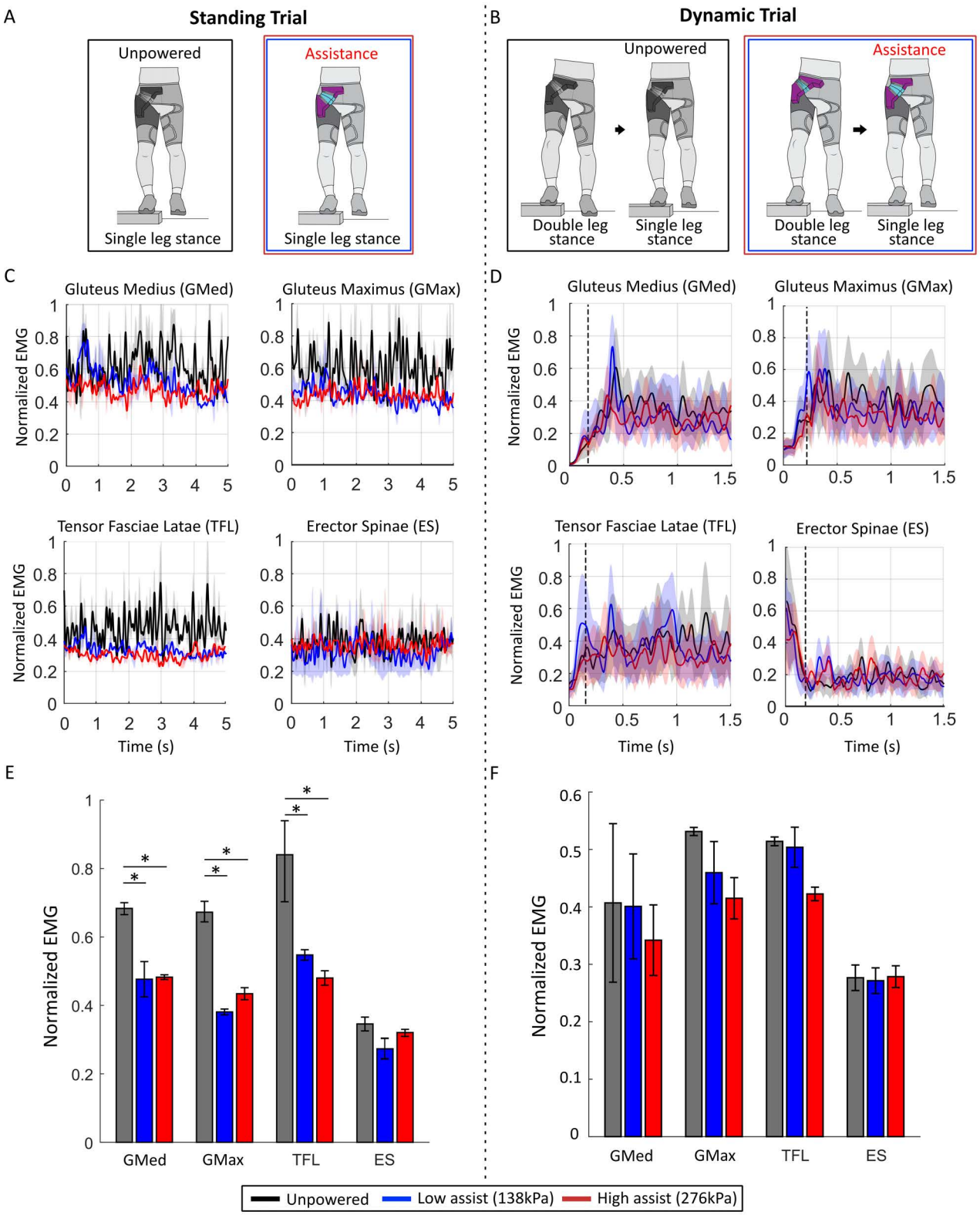

Fig. 5. The activities and conditions for the experimental protocol and the corresponding EMG measures. The unpowered (hip abduction actuator (HAA) was unpressurized) and assistance (HAA was pressurized) conditions are shown during single leg stance in standing trials (A) and during transition from double stance to single stance in dynamic trials (B). Normalized EMG linear envelopes GMed, GMax, TFL and ES activity (mean $\pm$ se) of the weighted limb during steady state single stance in standing trials (C), and during double leg stance to single leg transition in dynamics trials (D).The corresponding average normalized EMG linear envelopes (MEAN $\pm$ SD) for standing (E) and dynamic trials (F). * $p < .05$.

fied, low-pass filtered (fourth-order low-pass Butterworth, 12 Hz) to obtain linear envelopes and normalized by peak values across trials and conditions for each muscle. The normalized EMG linear envelopes for standing and dynamic trials were depicted in Fig. 5C and 5D respectively.

C. Statistical analysis

Repeated measure analysis of variance (ANOVA) for three conditions (unpowered, low assist and high assist) and two trials (standing and dynamic) were used on each dependent variable to identify differences with statistically significant effects. Paired t-tests were conducted to test if the changes in EMG, force, and kinematic measures between conditions within trials were different ($\alpha < 0.05$).

D. Testing results

In standing trials, compared to unpowered condition average normalized EMG linear envelopes from GMed, GMax and TFL on the weighted limb were reduced in low assist (29%, p = .036, 35%, p = .009 and 43%, p = .043, respectively) and high assist (30%, p = .005, 43%, p = .017 and 37%, p = .034, respectively) (Fig. 5E). For ES, no significant differences were observed in low assist (p= .173) and high assist (p = .737) compared to unpowered condition. During dynamic trials, there was no significant difference in average normalized EMG measures between conditions (p > .05), but a decreasing trend was observed for GMed, GMax and TFL with increased level of assistance (Fig. 5F).

The higher peak handrail forces in standing trials compared to dynamic trials could be from the increased difficulty of maintaining balance for longer time intervals. Nonetheless, the mean peak vertical force measured from the handrails ($F_{handrail}$) did not exceed 10 N for each condition and trial (Table I) and no significant difference was observed between conditions in standing (p = 0.699) and dynamic (p = 0.511) trials. No statistical difference was observed in pelvis roll range of motion and the peak toe height measures of the unweighted limb between conditions within trials as shown in Table I. The low handrail forces and the low amount of pelvis and toe movement suggest the participant did not use the handrail for weight support and did not make additional postural adjustments for loss of balance.

V. Conclusion and future work

In this paper, we presented a preliminary design and evaluation of a soft inflatable wearable robot for hip abductor assistance. The proposed device was constructed of lightweight textile components fashioned into a wearable suit. This suit was divided into three pieces: an anchoring sleeve established a tight connection with the body, and an actuating sleeve and thigh wrap aligned the actuator with the hip joint. A textile-based, pneumatically actuated hip abduction actuator (HAA) was attached with zippers to inflatables support beams, which were sewn to the suit to transmit torque to the body. Device characterization on a custom anthropometric test mannequin indicates the presented soft robotic device can deliver up to 16% of peak biological hip moment with 345 kPa. Experiments on a healthy individual (N=1) were conducted to evaluate the support provided by the proposed device. The results showed reduction in abductor muscle activity (GMed, GMax, and TFL) in single leg standing trials. In dynamic trials, there was a decreasing trend in abductor muscle activity with increased level of assistance. The preliminary results on a single participant demonstrate the proposed inflatable wearable device is capable of providing medial lateral support in a standing context and could also be beneficial for dynamic contexts.

The difference in reduction of EMG signal between standing and dynamic trials might be explained by the difficulty of synchronizing dynamic assistance with human motion. Furthermore, the slow inflation time of the HAA limited the rate of assistance that could be applied, which may have negatively impacted dynamic testing.

Future work on this device will investigate optimal design of the hip abduction actuator (HAA) and the support beams. Different geometry of the HAA will be investigated to provide higher torque assistance with lower pressure to allow the pump and power supply to be lighter and eventually portable. Additionally, alternate anchoring approaches will be pursued to reduce component migration relative to the body. To control the device during walking, the HAA needs to inflate and deflate quickly during single support phase (20-60% of gait cycle) of the targeted leg. To achieve this, we will investigate approaches to optimize the response time of the actuator. Further studies will be conducted to analyze how the torque provided by the device affects the kinematics of gait in both the frontal and sagittal plane. In addition, we plan to integrate pneumatic valves and IMUs to design a controller for dynamic torque assistance during locomotion.

ACKNOWLEDGMENT

The authors would like to thank Dr. Cameron Hohimer and Ciaran O'Neill for their assistance with the collection of device data, and Sarah Sullivan and Dr. Franchino Porciuncula with the IRB protocol.

References

[1] C. Living, "U.S. Department of Health and Human Services: Administration of Community Living & Administration of Aging - 2018 Profile of Older Americans," no. April, pp. 1–20, 2018.

[2] M. Rantakokko, M. Mänty, and T. Rantanen, "Mobility decline in old age," *Exercise and sport sciences reviews*, vol. 41, no. 1, pp. 19–25, 2013.

[3] K. Wilhelmson, C. Andersson, M. Waern, and P. Allebeck, "Elderly people's perspectives on quality of life," *Ageing and Society*, vol. 25, no. 4, pp. 585–600, 2005.

[4] S. Lin, K. Chang, H. Lee, Y. Yang, and J. Tsauo, "Problems and fall risk determinants of quality of life in older adults with increased risk of falling," *Geriatrics & gerontology international*, vol. 15, no. 5, pp. 579–587, 2015.

[5] S. S. Vaapio, M. J. Salminen, A. Ojanlatva, and S.-L. Kivelä, "Quality of life as an outcome of fall prevention interventions among the aged: a systematic review," *The European Journal of Public Health*, vol. 19, no. 1, pp. 7–15, 2009.

[6] A. F. Ambrose, G. Paul, and J. M. Hausdorff, "Risk factors for falls among older adults: A review of the literature," *Maturitas*, vol. 75, no. 1, pp. 51–61, 2013. [Online]. Available: http://dx.doi.org/10.1016/j.maturitas.2013.02.009

[7] B. H. Alexander, F. P. Rivara, and M. E. Wolf, "The cost and frequency of hospitalization for fall-related injuries in older adults." *American journal of public health*, vol. 82, no. 7, pp. 1020–1023, 1992.

[8] M. E. Tinetti, "Preventing falls in elderly persons," *New England journal of medicine*, vol. 348, no. 1, pp. 42–49, 2003.

[9] A. A. Vandervoort, "Aging of the human neuromuscular system," *Muscle and Nerve*, vol. 25, no. 1, pp. 17–25, 2002.

[10] J. Bae, C. Siviy, M. Rouleau, N. Menard, K. O'Donnell, I. Geliana, M. Athanassiu, D. Ryan, C. Bibeau, and L. Sloot, "A lightweight and efficient portable soft exosuit for paretic ankle assistance in walking after stroke," in *2018 IEEE International Conference on Robotics and Automation (ICRA)*. IEEE, 2018, pp. 2820–2827.

[11] A. B. Zoss, H. Kazerooni, and A. Chu, "Biomechanical design of the Berkeley lower extremity exoskeleton (BLEEX)," *IEEE/ASME Transactions on Mechatronics*, vol. 11, no. 2, pp. 128–138, 2006.

[12] H. Kazerooni, A. Chu, and R. Steger, "That which does not stabilize, will only make us stronger," *The International Journal of Robotics Research*, vol. 26, no. 1, pp. 75–89, 2007.

[13] A. J. Young and D. P. Ferris, "State of the art and future directions for lower limb robotic exoskeletons," *IEEE Transactions on Neural Systems and Rehabilitation Engineering*, vol. 25, no. 2, pp. 171–182, 2016.

[14] A. Kapsalyamov, P. K. Jamwal, S. Hussain, and M. H. Ghayesh, "State of the Art Lower Limb Robotic Exoskeletons for Elderly Assistance," *IEEE Access*, vol. 7, pp. 95 075–95 086, 2019.

[15] S. Jezernik, G. Colombo, T. Keller, H. Frueh, and M. Morari, "Robotic orthosis lokomat: A rehabilitation and research tool," *Neuromodulation: Technology at the neural interface*, vol. 6, no. 2, pp. 108–115, 2003.

[16] K. Seo, J. Lee, Y. Lee, T. Ha, and Y. Shim, "Fully autonomous hip exoskeleton saves metabolic cost of walking," *Proceedings - IEEE International Conference on Robotics and Automation*, vol. 2016-June, no. September, pp. 4628–4635, 2016.

[17] A. N. Spring, J. Kofman, and E. D. Lemaire, "Design and evaluation of an orthotic knee-extension assist," *IEEE Transactions on Neural Systems and Rehabilitation Engineering*, vol. 20, no. 5, pp. 678–687, 2012.

[18] J. A. Blaya and H. Herr, "Adaptive Control of a Variable-Impedance Ankle-Foot Orthosis to Assist Drop-Foot Gait," *IEEE Transactions on Neural Systems and Rehabilitation Engineering*, vol. 12, no. 1, pp. 24–31, 2004.

[19] J. Kim, G. Lee, R. Heimgartner, D. A. Revi, N. Karavas, D. Nathanson, I. Galiana, A. Eckert-Erdheim, P. Murphy, D. Perry, N. Menard, D. K. Choe, P. Malcolm, and C. J. Walsh, "Reducing the metabolic rate of walking and running with a versatile, portable exosuit," *Science*, vol. 365, no. 6454, pp. 668–672, 2019.

[20] S. Sridar, Z. Qiao, N. Muthukrishnan, W. Zhang, and P. Polygerinos, "A soft-inflatable exosuit for knee rehabilitation: Assisting swing phase during walking," *Frontiers Robotics AI*, vol. 5, no. MAY, pp. 1–9, 2018.

[21] S. Galle, P. Malcolm, S. H. Collins, and D. De Clercq, "Reducing the metabolic cost of walking with an ankle exoskeleton: interaction between actuation timing and power," *Journal of NeuroEngineering and Rehabilitation*, vol. 14, no. 1, pp. 1–16, 2017.

[22] M. G. Pandy, Y.-C. Lin, and H. J. Kim, "Muscle coordination of mediolateral balance in normal walking," *Journal of biomechanics*, vol. 43, no. 11, pp. 2055–2064, 2010.

[23] M. A. Schrager, V. E. Kelly, R. Price, L. Ferrucci, and A. Shumway-Cook, "The effects of age on medio-lateral stability during normal and narrow base walking," *Gait & posture*, vol. 28, no. 3, pp. 466–471, oct 2008.

[24] M. E. Johnson, M.-l. Mille, K. M. Martinez, G. Crombie, and M. W. Rogers, "Age-Related Changes in Hip Abductor and Adductor Joint Torques," vol. 85, no. April, pp. 593–597, 2004.

[25] P. Hardcastle and S. Nade, "The significance of the Trendelenburg test," *The Journal of bone and joint surgery. British volume*, vol. 67, no. 5, pp. 741–746, 1985.

[26] J. M. Hausdorff, D. A. Rios, and H. K. Edelberg, "Gait variability and fall risk in community-living older adults: A 1-year prospective study," *Archives of Physical Medicine and Rehabilitation*, vol. 82, no. 8, pp. 1050–1056, 2001.

[27] T. M. Owings and M. D. Grabiner, "Variability of step kinematics in young and older adults," *Gait & posture*, vol. 20, no. 1, pp. 26–29, 2004.

[28] T. Zhang, M. Tran, and H. H. Huang, "NREL-Exo: A 4-DoFs wearable hip exoskeleton for walking and balance assistance in locomotion," *IEEE International Conference on Intelligent Robots and Systems*, vol. 2017-Septe, pp. 508–513, 2017.

[29] L. Wang, S. Wang, E. H. Van Asseldonk, and H. Van Der Kooij, "Actively controlled lateral gait assistance in a lower limb exoskeleton," *IEEE International Conference on Intelligent Robots and Systems*, pp. 965–970, 2013.

[30] C. L. Dembia, A. Silder, T. K. Uchida, J. L. Hicks, and L. Delp, "Simulating ideal assistive devices to reduce the metabolic cost of walking with heavy loads," vol. 020405, pp. 1–25, 2017.

[31] B. T. Quinlivan, S. Lee, P. Malcolm, D. M. Rossi, M. Grimmer, C. Siviy, N. Karavas, D. Wagner, A. Asbeck, and I. Galiana, "Assistance magnitude versus metabolic cost reductions for a tethered multiarticular soft exosuit," *Sci. Robot*, vol. 2, no. 2, pp. 1–10, 2017.

[32] L. H. Sloot and M. M. van der Krogt, "Interpreting Joint Moments and Powers in Gait BT - Handbook of Human Motion." Cham: Springer International Publishing, 2018, pp. 625–643. [Online]. Available: https://doi.org/10.1007/978-3-319-14418-4_32

[33] D. E. Krebs, C. E. Robbins, L. Lavine, and R. W. Mann, "Hip biomechanics during gait," *Journal of Orthopaedic and Sports Physical Therapy*, vol. 28, no. 1, pp. 51–59, 1998.

[34] J. Chung, R. Heimgartner, C. T. O'Neill, N. S. Phipps, and C. J. Walsh, "ExoBoot, a Soft Inflatable Robotic Boot to Assist Ankle During Walking: Design, Characterization and Preliminary Tests," in *2018 7th IEEE International Conference on Biomedical Robotics and Biomechatronics (Biorob)*. IEEE, 2018, pp. 509–516.

[35] A. Roaas and G. B. Andersson, "Normal range of motion of the hip, knee and ankle joints in male subjects, 30–40 years of age," *Acta Orthopaedica Scandinavica*, vol. 53, no. 2, pp. 205–208, 1982.

[36] G. G. Simoneau, J. S. Ulbrecht, J. A. Derr, and P. R. Cavanagh, "Role of somatosensory input in the control of human posture," *Gait & posture*, vol. 3, no. 3, pp. 115–122, 1995.